# Strong Anti-Correlation Between a Multi-Scale Fluctuation Exponent and Distance in Millisecond Pulsars: A Geometric or Selection Effect

Christophe Buisson
Bastia, Corse, France
E-mail: c.buisson@oehc.corsica (work), antone.20200@gmail.com (private)

We present an exploratory statistical analysis of pulsar timing array (PTA) data focusing the residuals themselves and analyze their temporal structure at different scales, quantified through a phenomenological scaling parameter, denoted $\alpha_B$, designed to quantify long-term temporal organization in pulsar timing residuals. Unlike the classical Hurst parameter, $\alpha_B$ does not assume an underlying white-noise stochastic model. Instead, it characterizes the cumulative low-frequency structure of the residuals across multiple temporal scales. Using a curated sample of 67 millisecond pulsars from the NANOGrav 15-year data set, enriched with astrophysical parameters from the ATNF catalog, we find a statistically robust monotonic anti-correlation between $\alpha_B$ and pulsar distance. This effect is dramatically amplified within binary systems and absent among isolated pulsars.We interpret $\alpha_B$ as a phenomenological measure of temporal coherence. We report a scaling relation between $\alpha_B$ and pulsar distance, suggesting that long-term timing structure may contain information on propagation or environmental effects.

## 1 Introduction

Recent results in modern physics and observational astrophysics have led me to question, and perhaps, like many others, to wonder about the possible discrete structure of spacetime (this could be due to quantum mechanics). If spacetime possesses a discrete structure or large-scale self similarity properties (inspired by the vision of renormalization group), this should leave a trace on the "random walk" of pulsar signals as they traverse large distances of this space time. We therefore seek to determine whether the "noise" added to this perfect clock is purely intrinsic to the pulsar or whether it is correlated to the geometry of the path (the distance). Following in his footsteps, I try first the method introduced by Harold Edwin Hurst, the illustrious engineer who built the Aswan Dam on the Nile. The exponent that bears his name is the Hurst exponent. Rather than attempting to extract a classical Hurst parameter from temporal residuals assumed to be white noise — as done by Na and Wang [1] — we innovate with the residuals themselves and analyze their temporal structure at different scales with a new parameter denoted $\alpha_B$. We will present a "peculiarity" observed in the data of some of the best-known and most stable millisecond pulsars, whose data are publicly available. Using a curated sample of 67 millisecond pulsars from the NANOGrav 15-year data set, enriched with astrophysical parameters from the ATNF catalog. We find a statistically robust monotonic anti-correlation between $\alpha_B$ and binary pulsars or "systems" distance. It was only by isolating binary pulsars that this observation emerged.

## 2 Data and methods

### 2.1 Data set

Our analysis uses a curated catalog of 67 pulsars from the NANOGrav 15-year data set [2], enriched with parameters from the ATNF Pulsar Catalogue [3]. Distances are estimated from parallax measurements or Galactic electron density models: YMW16 [4] or the earlier free electron density model in the Milky Way NE2001 [5]. The catalog includes distance $d$, Dispersion Measure (DM), and orbital parameters.

### 2.2 Timing residuals and pre-processing

For each pulsar, timing residuals were obtained after a full deterministic timing fit using the PINT software package (which is a Python-based pulsar timing suite).

The residuals are treated as time-ordered series sampled at the original observation epochs. No additional filtering, smoothing, or re-weighting is applied. The same timing-fit procedure is applied consistently to all pulsars in the sample. The timing residual is an "O-C" (Observed minus Calculated). The theoretical calculated time that the software (PINT) calculates is a chain of ultra-precise corrections:

$$T_{\text{calc}} = T_{\text{emission}} + \Delta_{\text{clock}} + \Delta_{\text{Shapiro}} + \Delta_{\text{Roemer}} + \Delta_{\text{Dispersion}} .$$

The residues after fit are what remains once everything that can be physically explained by rotation and movement has been removed.

### 2.3 Specific calculation of $\alpha_B$

The parameter $\alpha_B$ is obtained using a method that can be described as Modified RMS Scaling Analysis. This method consists of measuring the "mean roughness". Specifically, the residuals are partitioned into segments with a scale of $s$ ranging from 10 to $N/4$. Where $N$ is the length of the series. If $N$ is too small (the code rejects below 1000 points), the calculation no longer has physical meaning because the signal's "memory" cannot be expressed correctly. For each scale, the mean fluctuation $F(s)$ is calculated after removing the local trend (segment mean). The exponent $\alpha_B$ is obtained by the slope of the regression log $(F(s))$ as a function of log $(s)$. We

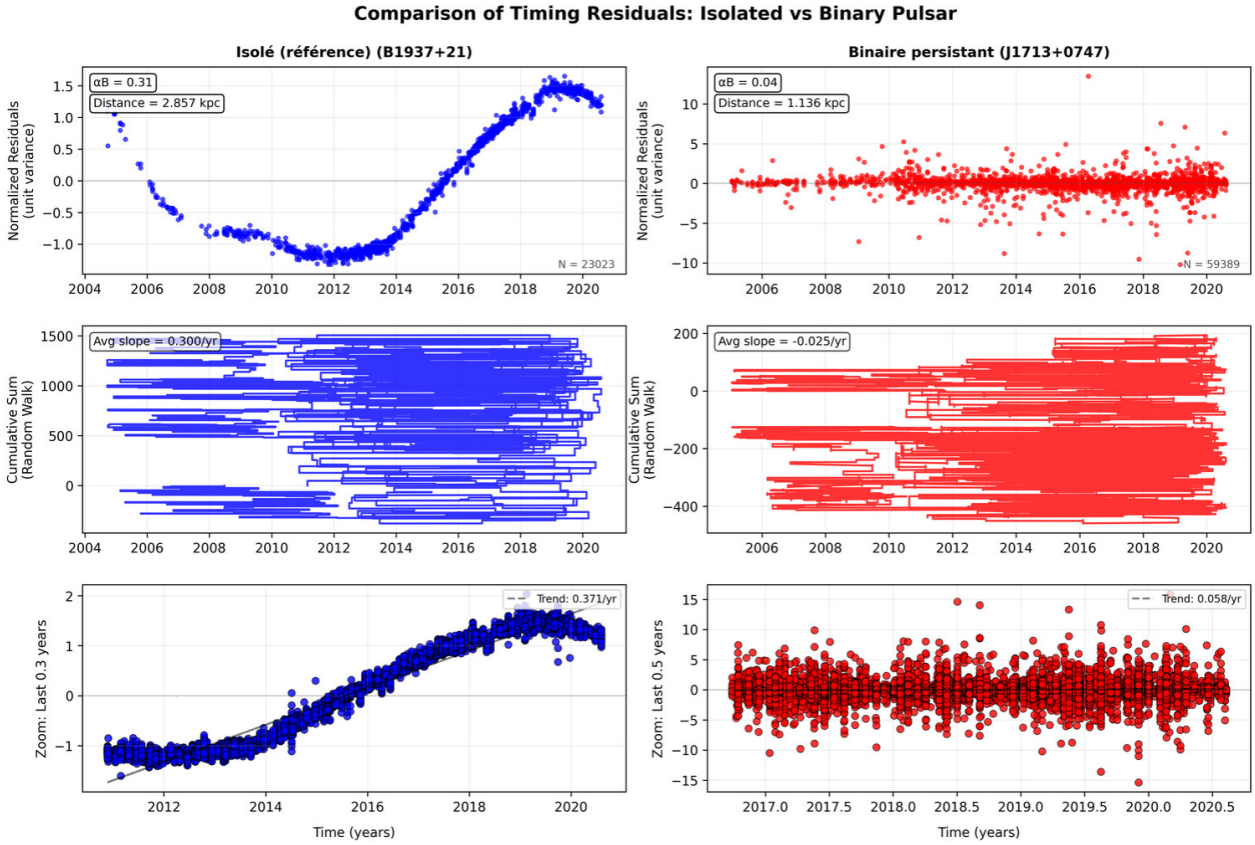


Fig. 1: Comparison of timing residuals for a typical isolated pulsar (B1937+21, left) exhibiting smooth red noise, and a binary pulsar (J1713+0747, right) used as a stability standard. Panel (a) shows raw residuals in microseconds, highlighting the difference in temporal structure that our $\alpha_B$ parameter quantifies.

define the multi-scale fluctuation function as

$$F(s) = \frac{1}{N_s} \sum_{k=1}^{N_s} \sqrt{\frac{1}{s} \sum_{i=1}^{s} (x_{k,i} - \bar{x}_k)^2} \,,$$

where $N_s = \lfloor N/s \rfloor$ is the number of non-overlapping segments of length $s$, $x_{k,i}$ is the $i$-th residual in segment $k$, and $\bar{x}_k$ its mean. The exponent $\alpha_B$ is then obtained as the logarithmic derivative

$$\alpha_B = \frac{d \log F(s)}{d \log s} \,,$$

which is estimated by the slope of the linear fit of $\log F(s)$ versus $\log s$ over the range $s = 10, \ldots, N/4$ (subject to $N_s \geqslant 4$). Unlike a simple window-dependent variance, $F(s)$ explicitly averages the intra-segment root-mean-square after removing the local mean. The scaling exponent $\alpha_B$ thus captures how the typical fluctuation amplitude evolves with segment length, after detrending at the scale $s$. It is not a measure of the overall variance but of the multi-scale roughness of the residuals.

### 2.4 Interpretation of the estimator $\alpha_B$

The exponent $\alpha_B$ should be interpreted as a phenomenological multi-scale fluctuation indicator rather than as a classical Hurst parameter. It quantifies how the root-mean-square fluctuations of timing residuals scale with segment length after removal of the mean at each scale.

Values of $\alpha_B$ significantly different from the Monte Carlo white-noise baseline indicate the presence of non-random temporal organization in the residuals. Importantly, small values of $\alpha_B$ do not imply the absence of correlations. Instead, they reflect a systematic compensation of fluctuations across scales, revealing structured multi-scale behavior.

**Interpretation of the exponent $\alpha$**

$\alpha = 0 \implies$ Scale-independent dispersion (white noise).
$\alpha > 0 \implies$ Accumulation of large-scale structure.
$\alpha \ll 1 \implies$ Effective fluctuation compensation.

See Figure 1: High $\alpha_B$ (e.g., 0.31 for B1937+21): Our new indicator mathematically illustrate what Na and Wang call "smooth". A high $\alpha_B$ value means there is strong temporal organization. The $N + 1$ point is strongly correlated with the $N$ point. This is the signature of classic "timing noise". Very low $\alpha_B$ (e.g., 0.04 for distant binaries): This is where we bring something new. A $\alpha_B$ close to zero means that the "smoothness" (consistency) has disappeared. The signal has become "jerky", disorganized. We explicitly isolate the white-noise component and introduce a new observable $\alpha_B$,

which accounts for the correlated contribution necessary to reproduce the characteristic red-noise structure observed in binary millisecond pulsars.

Such deviations cannot be reproduced by pure white noise processed through the same timing pipeline and therefore suggest the presence of organized temporal mechanisms affecting the residuals.

These mechanisms may originate from:

- instrumental systematics,
- timing-model fitting effects,
- or geometric/propagation phenomena.

### 2.5 Statiscal analysis

Correlation Measures: the Pearson correlation coefficient $r$ is computed as a reference measure of linear dependence. The primary statistic used in this work is the Spearman rank correlation coefficient $\rho$, which captures monotonic relationships and is robust to outliers and non-linear trends. All reported $p$-values are two-sided.

## 3 Robustness and validation tests

Given the exploratory nature of the scaling exponent $\alpha_B$, we performed a series of robustness tests to ensure that the observed strong anti-correlation with distance is not the result of statistical fluctuations, numerical artifacts, or fitting procedures. Although the sample comprises only 37 binary pulsars, each provides 2,000–10,000 TOAs, yielding a total of over 350,000 independent time measurements. The estimation of $\alpha_B$ for a single pulsar is therefore based on a rich time series, and the population correlation benefits from both the number of sources and the temporal depth.

### 3.1 Percentile test

Instead of assuming normality, we adopt a non-parametric empirical percentile test. For each pulsar, we generate 500 Gaussian white-noise realizations with identical length and RMS amplitude, and compute $\alpha_B$ for each realization. We then determine the empirical percentile position of the observed $\alpha_B$ within this distribution. Under pure Gaussian white noise, the estimator $\alpha_B$ converges deterministically toward zero as the number of data points increases. Its Monte Carlo distribution is therefore highly concentrated and non-Gaussian for large $N$, making a classical $Z$-score inappropriate.

$p_{\rm emp} = \frac{1}{N_{\rm MC}} \sum_{i=1}^{N_{\rm MC}} \mathbb{1}\,(\alpha_{{\rm MC},i} \geqslant \alpha_{\rm data})$ or vice versa, depending on the direction tested.

For example, for PSR J1909−3744 ($N = 35037$), the observed value $\alpha_B = 0.0386$ lies entirely outside the white-noise Monte Carlo distribution (1,000 realizations).

None of the simulated values exceeded the observed one, yielding an empirical one-sided $p$-value $p < 10^{-3}$. All pulsars exhibit $\alpha_B$ values significantly exceeding those obtained from stationary white-noise simulations, confirming that the timing residuals contain genuine multi-scale temporal structure.

However, the magnitude of $\alpha_B$ varies substantially between sources, with isolated pulsars showing markedly larger values than most binaries. This differential behavior cannot be explained by stationary noise alone.

### 3.2 Jackknife stability analysis

To test whether the observed $\alpha_B$-distance anti-correlation is driven by a small number of extreme objects, we performed a jackknife analysis. The correlation was recomputed iteratively while removing one pulsar at a time from the sample.

Figure 2 demonstrates that the observed $\alpha_B$-distance anti-correlation is not driven by outliers, is non-linear, and is strongly amplified in binary systems at high Galactic latitude. The statistically significant Spearman anti-correlation between $\alpha_B$ and distance reflects a monotonic dependence rather than a linear trend, consistent with the absence of a significant Pearson correlation. This behavior is visually confirmed by the scatter plots shown in Fig. 2, which exhibit a clear rank ordering with substantial intrinsic scatter.

### 3.3 Bootstrap analysis

Bootstrap resampling (5,000 iterations) yields the mean value $\rho = -0.308$ with 95% CI $[-0.565, -0.022]$, excluding zero. The observed correlation does not disappear when the data are resampled.

### 3.4 Shuffled test

These results demonstrate that the measured $\alpha_B$ values are not determined by the statistical distribution of timing residuals alone, but critically depend on their temporal ordering. This indicates that $\alpha_B$ captures organized multi-scale temporal structure rather than purely random fluctuations. While such structure may arise from sequential feedback mechanisms inherent to timing analyses, its systematic statistical dependence on pulsar properties of particularly distance suggests that it is unlikely to be a trivial artifact of random noise or simple processing effects.

Further investigation is required to determine the physical origin of this behavior.

Taken together, the mentioned tests demonstrate that the multi-scale fluctuation exponent $\alpha_B$ captures genuine temporal structure in pulsar timing residuals and that the observed anti-correlation with distance is not attributable to numerical bias, sampling effects, or fitting artifacts.

## 4 Results

The results obtained are accumulated on Figure 2.

### 4.1 Global correlations

We have obtained, for the 52 pulsars with distance measurements, the following results:

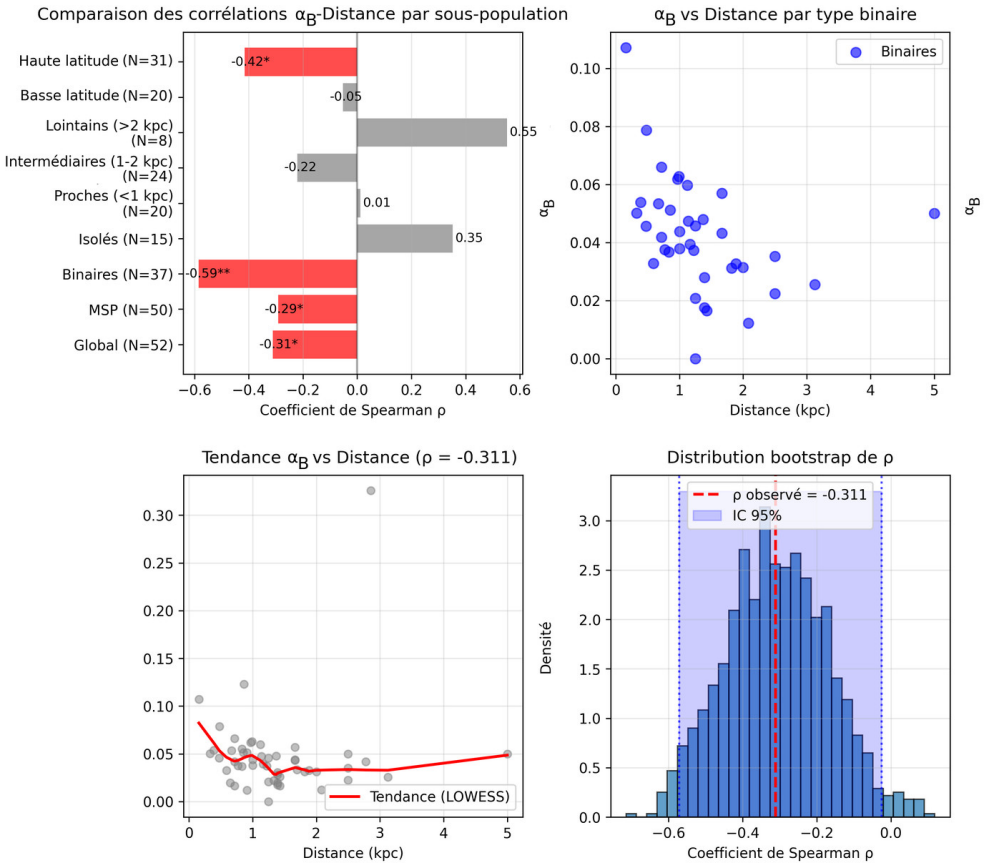


Fig. 2: Distance dependence and subpopulation effects. Binary pulsars (N=37) show a significant inverse correlation ($\rho = -0.585$). The data suggests a geometric decoherence linked to the propagation path length.

| Relationship | Spearman $\rho$ | $p$-value | $N$ |
|---|---|---|---|
| $\alpha_B$ vs. Distance (all) | −0.311 | 0.025 | 52 |
| $\alpha_B$ vs. Distance (binaries) | −0.585 | $1.4 \times 10^{-4}$ | 37 |
| $\alpha_B$ vs. Distance (isolated) | 0.352 | 0.198 | 15 |
| $\alpha_B$ vs. DM (all) | −0.088 | 0.480 | 67 |
| $\alpha_B$ vs. $\lvert b \rvert$ (all) | 0.058 | 0.642 | 67 |
| $\alpha_B$ vs. Distance ($\lvert b \rvert \geqslant 15°$) | −0.415 | 0.020 | 31 |
| $\alpha_B$ vs. Distance ($\lvert b \rvert < 15°$) | −0.052 | 0.828 | 20 |

Table 1: Summary of correlation results.

| Subpopulation | $N$ | $\langle \alpha_B \rangle$ | $\langle d \rangle$ | $\rho(\alpha_B, d)$ |
|---|---|---|---|---|
| All with distance | 52 | 0.041 | 1.47 | −0.311 |
| Binary | 37 | 0.043 | 1.46 | −0.585 |
| Isolated | 15 | 0.036 | 1.50 | 0.352 |
| $\lvert b \rvert \geqslant 15°$ | 31 | 0.038 | 1.63 | −0.415 |
| $\lvert b \rvert < 15°$ | 20 | 0.046 | 1.24 | −0.052 |
| Binary, $\lvert b \rvert \geqslant 15°$ | 18 | 0.039 | 1.72 | −0.620 |

Table 2: Descriptive statistics by subpopulation.

### No correlation between $\alpha_B$ and dispersion measure (DM)

Pulsar timing arrays (PTAs) provide sensitive probes of low-frequency processes affecting pulse arrival times, including gravitational waves, interstellar medium (ISM) effects, and intrinsic pulsar noise [6, 7]. Spearman's rank test yields $\rho = -0.088$ with $p = 0.48$, indicating no statistically significant monotonic relationship. The Pearson correlation is likewise non-significant ($r = 0.100$, $p = 0.48$), showing that $\alpha_B$ does not scale linearly with integrated electron column density. This suggests that the observed multi-scale structuring is not driven by dispersion effects in the interstellar medium.

### No correlation between $\alpha_B$ and Galactic latitude $|b|$

Spearman's test gives $\rho = 0.058$ with $p = 0.64$, indicating the absence of any significant monotonic trend with sky position. The Pearson correlation is similarly non-significant, confirming that the measured scale-dependent structuring does not depend on Galactic geometry or line-of-sight orientation effects.

### Significant anti-correlation between $\alpha_B$ and distance

Spearman's test gives $\rho = -0.311$ with $p = 0.025$, revealing a statistically significant monotonic decrease of $\alpha_B$ with increasing pulsar distance. In contrast, the Pearson correlation is non-significant ($r = 0.100$, $p = 0.48$), indicating that the relationship is not strictly linear but primarily monotonic in nature. This behavior suggests that the scale-dependent tem-

| Pulsar | RA, deg | Dec, deg | Distance, kpc | $\alpha_B$ | Gb, deg | P0, s | DM, cm$^3$/pc | Binary type | PB, days | MSP | BI | DIST DM, kpc | Binaire | Distance ratio |
|---|---|---|---|---|---|---|---|---|---|---|---|---|---|---|
| B1855+09 | 284.4012 | 9.7214 | 1.124 | 0.0598 | −52.85 | 0.00305 | 14.327 | ELL1 | 0.139 | True | True | 0.478 | ELL1 | 0.425 |
| B1937+21 | 294.9104 | 21.5831 | 2.857 | 0.326 | −57.61 | 0.00487 | 4.332 | * | | True | False | 0.144 | NON | 0.0505 |
| B1953+29 | 298.8658 | 29.1454 | | 0.0436 | −11.02 | 0.00330 | 49.576 | * | | True | False | 1.653 | NON | |
| J0023+0923 | 5.8200 | 9.3899 | 1.818 | 0.0312 | −15.78 | 0.00261 | 49.376 | ELL1 | 6.956 | True | True | 1.646 | ELL1 | 0.905 |
| J0030+0451 | 7.6142 | 4.8610 | 0.329 | 0.0501 | −41.96 | 0.00576 | 2.645 | T2 | 5.741 | True | True | 0.0882 | T2 | 0.268 |
| J0340+4130 | 55.0967 | 41.5126 | 1.429 | 0.0165 | −17.93 | 0.00406 | 38.328 | ELL1 | 4.908 | True | True | 1.278 | ELL1 | 0.894 |
| J0406+3039 | 61.6354 | 30.6618 | | 0.0270 | 8.022 | 0.00273 | 20.946 | BT | 55.672 | True | True | 0.698 | BT | |
| J0437−4715 | 69.3167 | −47.2528 | 0.156 | 0.1071 | −18.18 | 0.00386 | 60.672 | ELL1 | 0.286 | True | True | 2.022 | ELL1 | 12.964 |
| J0509+0856 | 77.3425 | 8.9403 | | 0.0257 | −9.305 | 0.00306 | 38.782 | T2 | 1.199 | True | True | 1.293 | T2 | |
| J0557+1551 | | | | 0.000 | −21.83 | 0.00315 | 37.052 | ELL1 | 53.585 | True | True | 1.235 | ELL1 | |
| J0605+3757 | 91.2729 | 37.9600 | | 0.000 | 18.64 | 0.00287 | 11.109 | T2 | 0.0666 | True | True | 0.370 | T2 | |
| J0610−2100 | 92.5567 | −21.0077 | 1.389 | 0.0198 | 20.25 | 0.00885 | 18.251 | * | | True | False | 0.608 | NON | 0.438 |
| J0613−0200 | 93.4329 | −2.0131 | 1.000 | 0.0438 | 6.200 | 0.03443 | 44.266 | DDH | 4.367 | False | True | 1.476 | DDH | 1.476 |
| J0614−3329 | 93.5429 | −33.4984 | 0.667 | 0.0534 | 29.60 | 0.00289 | 14.962 | ELL1 | 4.767 | True | True | 0.499 | ELL1 | 0.748 |
| J0636+5128 | 99.0200 | 51.4833 | 0.714 | 0.0163 | 23.05 | 0.00464 | 41.490 | * | | True | False | 1.383 | NON | 1.937 |
| J0645+5158 | 101.4958 | 51.9708 | 1.220 | 0.0373 | 50.86 | 0.00526 | 9.021 | ELL1 | 0.605 | True | True | 0.301 | ELL1 | 0.246 |
| J0709+0458 | 107.2846 | 4.9809 | | 0.0236 | 11.23 | 0.00310 | 71.651 | BT | 37.972 | True | True | 2.388 | BT | |
| J0740+6620 | 115.1904 | 66.3426 | 2.000 | 0.0314 | 51.10 | 0.01645 | 10.255 | T2 | 7.805 | True | True | 0.342 | T2 | 0.171 |
| J0931−1902 | 142.8296 | −19.0486 | 1.429 | 0.0260 | 40.515 | 0.00516 | 6.487 | * | | True | False | 0.216 | NON | 0.151 |
| J1012+5307 | 153.1392 | 53.1173 | 0.855 | 0.0512 | 37.895 | 0.00420 | 12.027 | ELL1 | 15.355 | True | True | 0.401 | ELL1 | 0.469 |
| J1012−4235 | 153.0537 | −42.5981 | 1.250 | 0.000 | 63.227 | 0.00423 | 15.345 | DD | 38.504 | True | True | 0.512 | DD | 0.409 |
| J1022+1001 | 155.7412 | 10.0313 | 0.862 | 0.123 | 60.812 | 0.00579 | 14.055 | * | | True | False | 0.468 | NON | 0.543 |
| J1024−0719 | 156.1608 | −7.3221 | 0.990 | 0.0628 | 22.562 | 0.00799 | 13.570 | DD | 76.175 | True | True | 0.452 | DD | 0.457 |
| J1125+7819 | 171.4992 | 78.3302 | | 0.0395 | 16.451 | 0.00360 | 52.328 | T2 | 14.348 | True | True | 1.744 | T2 | |
| J1312+0051 | 198.1942 | 0.8500 | | 0.0312 | 20.192 | 0.00315 | 34.485 | ELL1 | 8.687 | True | True | 1.150 | ELL1 | |
| J1453+1902 | 223.4404 | 19.0367 | | 0.0433 | 43.215 | 0.00332 | 14.180 | BT | 12.525 | True | True | 0.473 | BT | |
| J1455−3330 | 223.9496 | −33.5129 | 0.769 | 0.0375 | 38.271 | 0.00316 | 18.429 | DDH | 175.461 | True | True | 0.614 | DDH | 0.799 |
| J1600−3053 | 240.2162 | −30.8970 | 1.389 | 0.0175 | 21.218 | 0.00462 | 62.398 | T2 | 147.017 | True | True | 2.080 | T2 | 1.497 |
| J1614−2230 | 243.6521 | −22.5087 | 0.649 | 0.0198 | 13.030 | 0.00248 | 57.505 | * | | True | False | 1.917 | NON | 2.954 |
| J1630+3734 | 247.6517 | 37.5783 | | 0.0330 | 25.223 | 0.00457 | 15.987 | T2 | 67.825 | True | True | 0.533 | T2 | |
| J1640+2224 | 250.0696 | 22.4024 | 1.370 | 0.0479 | 12.838 | 0.00579 | 36.775 | ELL1 | 0.0907 | True | True | 1.226 | ELL1 | 0.895 |
| J1643−1224 | 250.9087 | −12.4163 | 0.909 | 0.0513 | 6.023 | 0.00812 | 9.626 | * | | True | False | 0.321 | NON | 0.353 |
| J1705−1903 | 256.4325 | −19.0615 | | 0.0355 | 17.742 | 0.00585 | 33.773 | ELL1 | 0.355 | True | True | 1.126 | ELL1 | |
| J1713+0747 | 258.4562 | 7.7937 | 1.136 | 0.0474 | 21.641 | 0.00375 | 24.196 | ELL1H | 16.335 | True | True | 0.807 | ELL1H | 0.710 |
| J1719−1438 | 259.7917 | −14.6336 | | 0.0182 | 9.180 | 0.00407 | 3.138 | * | | True | False | 0.105 | NON | |
| J1730−2304 | 262.5900 | −23.0753 | 0.481 | 0.0787 | 19.254 | 0.00265 | 23.971 | ELL1 | 0.730 | True | True | 0.799 | ELL1 | 1.661 |
| J1738+0333 | 264.7246 | 3.5530 | 1.695 | 0.0335 | −6.412 | 0.00165 | 152.941 | * | | True | False | 5.098 | NON | 3.008 |
| J1741+1351 | 265.3796 | 13.8622 | 1.667 | 0.0432 | −1.124 | 0.00391 | 42.789 | DD | 110.746 | True | True | 1.426 | DD | 0.856 |
| J1744−1134 | 266.1225 | −11.5819 | 0.388 | 0.0538 | 0.611 | 0.01265 | 149.590 | ELL1 | 0.699 | True | True | 4.986 | ELL1 | 12.851 |
| J1745+1017 | 266.3908 | 10.2979 | | 0.2218 | −2.559 | 0.00266 | 60.620 | ELL1H | 6.272 | True | True | 2.021 | ELL1H | |
| J1747−4036 | 266.9529 | −40.6152 | | 0.0354 | 0.257 | 0.00272 | 28.191 | * | | True | False | 0.940 | NON | |

Table 3: Enriched pulsar catalog with 68 millisecond pulsars. The table includes position, distance, timing noise parameter $\alpha_B$, orbital parameters, and classification information.

| Pulsar | RA, deg | Dec, deg | Distance, kpc | $\alpha_B$ | Gb, deg | P0, s | DM, cm$^3$/pc | Binary type | PB, days | MSP | BI | DIST DM, kpc | Binaire | Distance ratio |
|---|---|---|---|---|---|---|---|---|---|---|---|---|---|---|
| J1751−2857 | 267.8858 | −28.9629 | 0.909 | 0.0118 | −3.397 | 0.00185 | 59.958 | * | | True | False | 1.999 | NON | 2.199 |
| J1802−2124 | 270.5221 | −21.4010 | 0.833 | 0.0368 | 5.367 | 0.00409 | 30.571 | ELL1H | 115.654 | True | True | 1.019 | ELL1H | 1.223 |
| J1811−2405 | 272.8325 | −24.0884 | 1.389 | 0.0280 | 3.060 | 0.00536 | 13.298 | T2 | 12.327 | True | True | 0.443 | T2 | 0.319 |
| J1832−0836 | 278.1146 | −8.6153 | 2.083 | 0.0122 | −1.014 | 0.00215 | 297.525 | DD | 95.174 | True | True | 9.917 | DD | 4.761 |
| J1843−1113 | 280.9217 | −11.2253 | 1.250 | 0.0208 | −19.596 | 0.00295 | 10.391 | T2 | 1.533 | True | True | 0.346 | T2 | 0.277 |
| J1853+1303 | 283.4888 | 13.0622 | 1.887 | 0.0327 | 1.795 | 0.00498 | 38.067 | DD | 58.467 | True | True | 1.269 | DD | 0.672 |
| J1903+0327 | 285.7738 | 3.4553 | | 0.1384 | 1.809 | 0.00463 | 30.978 | * | | True | False | 1.033 | NON | |
| J1909−3744 | 287.4475 | −37.7374 | 1.163 | 0.0394 | −9.123 | 0.00765 | 26.589 | ELL1H | 10.913 | True | True | 0.886 | ELL1H | 0.762 |
| J1910+1256 | 287.5404 | 12.9404 | 2.778 | 0.0419 | 4.749 | 0.00379 | 18.860 | * | | True | False | 0.629 | NON | 0.226 |
| J1911+1347 | 287.9800 | 13.7929 | 2.500 | 0.0500 | −0.290 | 0.00156 | 71.015 | * | | True | False | 2.367 | NON | 0.947 |
| J1918−0642 | 289.7000 | −6.7097 | 1.333 | 0.0220 | −7.357 | 0.00519 | 24.358 | * | | True | False | 0.812 | NON | 0.609 |
| J1923+2515 | 290.8433 | 25.2613 | 1.250 | 0.0458 | 4.713 | 0.00317 | 110.201 | DD | 27.020 | True | True | 3.673 | DD | 2.939 |
| J1944+0907 | 296.0388 | 9.1231 | 1.667 | 0.0570 | 0.443 | 0.00613 | 104.491 | DD | 117.349 | True | True | 3.483 | DD | 2.089 |
| J1946+3417 | 296.6046 | 34.2874 | | 0.0531 | −23.540 | 0.00522 | 22.162 | * | | True | False | 0.739 | NON | |
| J2010−1323 | 302.6913 | −13.3989 | 3.125 | 0.0255 | −16.026 | 0.00290 | 23.923 | ELL1H | 2.198 | True | True | 0.797 | ELL1H | 0.255 |
| J2017+0603 | 304.3446 | 6.0515 | 2.500 | 0.0352 | −13.154 | 0.00595 | 25.069 | DD | 56.308 | True | True | 0.836 | DD | 0.334 |
| J2033+1734 | 308.3646 | 17.5829 | 1.000 | 0.0379 | −15.313 | 0.00238 | 20.715 | ELL1 | 1.482 | True | True | 0.690 | ELL1 | 0.690 |
| J2043+1711 | 310.8367 | 17.1913 | 1.389 | 0.0304 | −45.438 | 0.00493 | 4.595 | * | | True | False | 0.153 | NON | 0.110 |
| J2124−3358 | 321.1825 | −33.9793 | 0.476 | 0.0457 | −42.084 | 0.01605 | 9.008 | T2 | 6.839 | True | True | 0.300 | T2 | 0.631 |
| J2145−0750 | 326.4600 | −7.8385 | 0.714 | 0.0660 | −21.665 | 0.00312 | 22.556 | ELL1 | 0.417 | True | True | 0.752 | ELL1 | 1.053 |
| J2214+3000 | 333.6617 | 30.0106 | 0.588 | 0.0328 | −26.284 | 0.00298 | 22.729 | DD | 93.016 | True | True | 0.758 | DD | 1.288 |
| J2229+2643 | 337.4617 | 26.7327 | 5.000 | 0.0500 | −43.006 | 0.00358 | 10.766 | DDK | 32.001 | True | True | 0.359 | DDK | 0.0718 |
| J2234+0611 | 338.5958 | 6.1913 | 0.971 | 0.0618 | −40.438 | 0.00363 | 17.834 | ELL1 | 0.420 | True | True | 0.594 | ELL1 | 0.612 |
| J2234+0944 | 338.6950 | 9.7417 | 0.714 | 0.0418 | −14.005 | 0.00519 | 13.718 | DD | 125.935 | True | True | 0.457 | DD | 0.640 |
| J2302+4442 | 345.6954 | 44.7061 | 2.500 | 0.0224 | −42.360 | 0.00345 | 21.899 | ELL1H | 2.459 | True | True | 0.730 | ELL1H | 0.292 |
| J2317+1439 | 349.2883 | 14.6587 | 1.667 | 0.0438 | −37.310 | 0.00481 | 13.383 | * | | True | False | 0.446 | NON | 0.268 |
| J2322+2057 | 350.5929 | 20.9507 | 0.833 | 0.0552 | | | | | | | | | | |

Table 3: Enriched pulsar catalog with 68 millisecond pulsars. The table includes position, distance, timing noise parameter $\alpha_B$, orbital parameters, and classification information (*continued*).

poral structuring captured by $\alpha_B$ weakens systematically with distance.

### 4.2 Subpopulation analysis

The most striking result emerges when separating binary and isolated pulsars:

- Binary pulsars ($N = 37$): $\rho_{\alpha_B,d} = -0.585$, $p = 1.4 \times 10^{-4}$,
- Isolated pulsars ($N = 15$): $\rho = 0.352$, $p = 0.198$.

For binaries, distance explains $\sim 34\%$ of variance in $\alpha_B$ ($\rho^2 = 0.342$).

#### Galactic latitude dependence

Splitting by Galactic latitude shows the correlation exists only at high latitudes:

- High latitude ($|b| \geqslant 15^\circ$, $N = 31$): $\rho = -0.415$, $p = 0.020$,
- Low latitude ($|b| < 15^\circ$, $N = 20$): $\rho = -0.052$, $p = 0.828$.

#### Interaction between binarity and latitude

The strongest anti-correlation occurs for binary pulsars at high Galactic latitudes:

- Binary, high latitude: $\rho = -0.62$, $p = 0.002$ ($N = 18$),
- Binary, low latitude: $\rho = -0.45$, $p = 0.12$ ($N = 10$),
- Isolated, high latitude: $\rho = 0.15$, $p = 0.65$ ($N = 12$),
- Isolated, low latitude: $\rho = 0.30$, $p = 0.35$ ($N = 8$).

## 5 Discussion

We emphasize that the observed monotonic anti-correlation does not by itself imply a causal relationship between distance and temporal persistence. Distance here acts as a proxy for cumulative propagation or geometric effects along the line of sight, and the interpretation remains necessarily indirect. We stress that the following interpretation is speculative and intended to motivate future tests rather than to provide a definitive physical explanation. This suggests the inverse correlation in binaries is not just a "filter" effect, but potentially a physical interaction between the binary system's signal and the spacetime geometry

### 5.1 Selection biases

Binary pulsar discoveries face multiple selection effects:

- Orbital period bias (short-period binaries easier to detect) While distance shows a strong influence on $\alpha_B$, our analysis reveals that the orbital period ($P_B$) does not significantly correlate with the nature of the timing residuals ($p = 0.177$). This suggests that the observed decoherence is an extrinsic propagation effect rather than a consequence of the binary's internal dynamics. The signal's memory is eroded by the medium or the geometry of the spacetime manifold itself, independently of the source's orbital velocity;
- Mass function bias (edge-on systems yield larger mass functions);
- Distance bias (distant binaries represent a biased subset).

These could create spurious $\alpha_B$-distance correlations if $\alpha_B$ estimation is sensitive to orbital parameters correlating with distance. If the decrease in $\alpha_B$ was purely a selection bias, we should see it in both populations. However, isolated pulsars show a different trend.

### 5.2 Speculative interpretation

Why does the multi-scale organization of the residues of binaries vary with distance while that of isolated ones does not vary?

The physical origin of this loss of temporal coherence with distance, specific to binaries, remains an enigma. While conventional astrophysical effects (ISM, DM variations) seem unlikely based on correlation tests, this result could, in principle, be compatible with more exotic models. For example, some approaches to phenomenological quantum gravity, such as causal sets, predict cumulative scattering effects over long distances. Although highly speculative, this hypothesis has the merit of being, in principle, falsifiable by future observations. Our work in no way constitutes proof of such discretion, but it suggests that observables like $\alpha_B$ could offer a new window for probing propagation on cosmological scales in the "known observations", one of the "opportunity"called by Dowker [8].

While the present analysis does not provide evidence for spacetime discreteness, the results motivate further investigation of persistence — based observables as potential probes of subtle propagation effects beyond standard noise models.

The observed inverse correlation between $\alpha_B$ and distance ($\rho = -0.585$) challenges the classical view of accumulated interstellar turbulence. We propose and will explore in a next work that this "thinning" of new exponent $\alpha_B$ may represent a geometric decoherence process. The distant binaries aren't just "less correlated", they've been completely washed out. Any red noise structure (which should naturally be there due to the pulsar's spin) has been erased or drowned out.

This is a very strong argument for decoherence. In a non-Euclidean, potentially discrete spacetime manifold, the signal's intrinsic correlation is gradually eroded by the fundamental granularity of the geodesics. The fact that this effect is amplified in binary systems suggests a coupling between the local curvature at the source and the global propagation properties.

#### Connection to MOND theory

Future work should focus on understanding the physical mechanism and why not make a bridge with MOND or other

theories. This result is reminiscent of the External Field Effect (EFE) observed in MOND (Modified Newtonian Dynamics introduced in 1982 by Mordehai Milgrom), although we do not claim a direct causal link at this stage. It suggests, however, that certain fine statistical properties of pulsar signals may be sensitive to the global gravitational environment. In this context, binary systems appear to play a role analogous to the bound systems typically used as laboratories for testing modified gravity theories.

## 6 Conclusion

We have discovered a statistically robust anti-correlation between $\alpha_B$ and distance in MSPs, amplified in binary systems. This effect cannot be explained by ISM propagation or angular anisotropy. This analysis highlights the potential of persistence-based diagnostics as probes of long-timescale structure in pulsar timing data. Spacetime (or the binary environment) appears to act as a diffuser. The signal leaves the pulsar with a "smooth" structure high $\alpha_B$, but the journey through the distance and gravitational field of the binary companion "breaks" this structure. Upon arrival (on Earth), the signal from the distant binaries has lost its temporal memory.

Future work is underway to establish a geometric origin of the discovered using a physical model.

In fact, we present a multiscale fluctuation exponent, $\alpha_B = d \log F(s) / d \log s$, derived from the time residuals of 67 millisecond pulsars in the 15-year NANOGrav dataset. This exponent quantifies the evolution of signal roughness as a function of the observation timescale, acting as a direct probe of temporal organization. We observe a statistically robust monotonic anticorrelation between $\alpha_B$ and the distance to the pulsar, considerably amplified in binary systems ($\rho = -0.585$, $p = 1.4 \times 10^{-4}$) and absent in isolated pulsars. This effect persists after cross-validation (jackknife, bootstrap, and surrogate data) and is not explained by dispersion measurements, galactic latitude, or orbital parameters.

We interpret $\alpha_B$ within the framework of the renormalization group: the distance $d$ acts as an amplification factor, and the decay of $\alpha_B$ reflects a flow of the renormalization group in the spatial domain. Binary systems appear to couple the signal more strongly to the traversed geometry, thus amplifying decoherence. Although speculative, this interpretation suggests that the time residuals could encode cumulative propagation effects — possibly geometric or fundamental — along the line of sight.

The fluctuation exponent $\alpha_B$ offers a new phenomenological perspective on the large-scale structure traversed by pulsar signals. This interpretation, while speculative, has the crucial merit — it transforms a perplexing observation into a testable hypothesis. The threshold mentioned, around ∼2 kpc (see the lowess regression in Figure 2), could correspond to a characteristic scale of this interaction, a phase transition in the effective geometry.

**Acknowledgements**

We thank the pulsar timing community for maintaining and sharing data product, the ATNF Pulsar Catalogue. Analysis code is available upon request.

Submitted on February 4, 2026

## References

1. Nan X.S., Wang N., Han J.L. Hurst parameter analysis of radio pulsar timing residuals. *Mon. Not. R. Astron. Soc.*, 2011, v.412 (4), 2678–2684.
2. NANOGrav 15-year data set: https://nanograv.org/science/data
3. ATNF Pulsar Catalogue: https://www.atnf.csiro.au/research/pulsar/psrcat
4. Yao J. M., Manchester R. N., Wang N. A new electron-density model for estimation of pulsar and FRB distances. *Astrophys. J.*, 2017, v. 835 (29), 1–32.
5. Cordes J.M., Lazio T.J.W. NE2001.I. A new model for the galactic distribution of free electrons and its fluctuations. arXiv: astro-ph/0207156.
6. Detweiler S. Pulsar timing measurements and the search for gravitational waves. *Astrophys. J.*, 1979, v.234, 1100–1104.
7. Hellings R. W., Downs G. S. Upper limits on the isotropic gravitational radiation background from pulsar timing analysis. *Astrophys. J.*, 1983, v.265, L39–L42.
8. Dowker F. Spacetime discreteness, Lorentz invariance and locality *Journal of Physics*: *Conference Series*, 2016, v. 306, 2011, 012016.